Wildfire Impacts on Annual Flood Peaks Across the Western United States

Guo Yu, Postdoc, Desert Research Institute, Las Vegas, NV, guo.yu@dri.edu

Julianne Miller, Research Scientist, Desert Research Institute, Las Vegas, NV, julie.miller@dri.edu

Sachiko Sueki, Assistant Research Scientist, Desert Research Institute, Las Vegas, NV, sachiko.sueki@dri.edu

Abstract

Wildfires can directly affect public health, the natural environment, and federal and state budgets. The indirect hydrologic impacts of wildfire, such as flooding and debris flows, can also be destructive. Despite the importance of the hydrologic impacts of wildfire, especially on post-fire flood events, their relationship to a wide range of climatological and geophysical settings is poorly understood. This study examines the post-fire streamflow dynamics of a number of watersheds across the western United States (US). In this study, we used US Geological Survey (USGS) annual peak flow and daily mean streamflow; precipitation and snowmelt from the North American Land Data Assimilation System version 2 (NLDAS-2) and NLDAS Variable Infiltration Capacity (NLDAS-VIC) simulations, respectively; and the Monitoring Trends in Burn Severity (MTBS) Project wildfire size and burn severity. We analyzed: 1) the different seasonalities of wildfire and annual peak flows, as well as the interval between a wildfire and the first subsequent flood; 2) changes in post-fire annual peak flows and their corresponding non-exceedance probability; 3) changes in runoff ratios for post-fire flood events; and 4) the relationship between post-fire flood impacts and the climatological and geophysical settings of watersheds. These analyses were applied to 714 watersheds across the western US that experienced at least one wildfire during the 1984-2020 period. The results show that the interval between a wildfire and the first subsequent flood varies across the western US, with the longest intervals occurring in high-latitude states, shorter intervals on the West Coast, and the shortest intervals in the arid Southwest. In general, peak flows during the first year after a wildfire are statistically significantly larger than pre-fire peak flows. This pattern is more obvious in smaller watersheds with larger percent burn areas. Consistently, post-fire runoff ratios were found to be larger than their pre-burn median values for small and medium watersheds (< 405 km2), especially in arid regions. In addition, the impacts of wildfire on flood behaviors (e.g., magnitudes and runoff ratios) were found to be minimal four to five years after wildfires. Finally, the empirical analyses performed in this study further support the study of wildfire impacts on regional flood frequency analysis.

1. INTRODUCTION

1.1 Background and Motivation

Wildfire is one of the most devastating natural hazards in the conterminous United States (CONUS), posing a threat to air quality, infrastructure, lives, and property. According to the National Interagency Fire Center (NIFC), annual-averaged wildfires in the United States (US) have burned 6.8 million acres with a suppression cost of $1.8 billion since 2010 (NIFC 2020). Because of warmer springs and longer and drier summers stemming from anthropogenic climate change, wildfires have become more frequent and larger in size over the western US since the 1980s (Westerling et al. 2006). This change in the hydroclimate caused forests in the western US to become more vulnerable to wildfire, which cannot be effectively mitigated by land management. This increasing trend in wildfire activity over the western US is projected to continue in the future as climate change enhances fuel aridity and vapor pressure deficit (e.g., Abatzoglou and Williams 2016; Jay et al. 2018).

In addition to the direct impacts of wildfires on ecosystems and human communities, wildfires can the hydrologic processes (e.g., Benavides-Solorio and MacDonald 2001; Cannon et al. 2001; Meyer et al. 2001). It is widely accepted that after a wildfire, water infiltration tends to decrease, producing both substantial overland flow and debris flows. DeBano et al. (1970) conducted an experiment to demonstrate that burning organic matter can create a hydrophobic layer below the soil surface, which results in water repellency. DeBano et al. (1979) further quantified the influence of soil temperature on soil hydrophobicity, providing insights into the post-fire soil hydrology. In addition to experiment-based studies, some observation-based studies show that wildfire can cause widespread development of water repellency in soils, which further increases peak flows, flood volumes, and catchment response ratios (e.g., Scott and Van Wyk 1990; Doerr et al. 2006).

Nevertheless, the hydrologic impacts of wildfire are complicated. Imeson et al. (1992) is one of the earliest studies that found that not all soils show a decreasing infiltration rate after wildfire, which contrasts with the infiltration theory. Ebel and Moody (2013) reviewed differences between infiltration theory and observations and argued that the traditional "decreasing infiltration" theory is insufficient to quantify infiltration rates in burned soils. A wildfire-induced ash layer on the soil surface can absorb water rapidly (Onda et al. 2008), whereas the underlying soil is water repellent because of the combined effects of hydrophobicity and hyper-dry conditions (Doerr et al. 2004; Moody and Ebel 2012). Increases in first-year runoff and peak flows are evident for watersheds encompassing a range of ecological regions in the US (Coombs and Melack 2013; Kinoshita and Hogue 2015; Loáiciga et al. 2001; Neary et al. 2005). However, other studies detected no significant changes in post-fire streamflows, which is attributable to natural annual variability (Aronica et al. 2002; Bart and Hope 2010; Townsend and Douglas 2000). This disparity among studies evaluating post-fire hydrology can be attributed to other modulating variables, including climate, soil and vegetation types, watershed morphology, and rainfall intensity after a wildfire (Moody et al. 2013).

Therefore, there is a critical need to examine post-fire streamflow dynamics, especially for flood events emanating from burned watersheds that encompass a broad spectrum of climatological and geophysical settings. Investigating the impacts of wildfire on floods over large scales will provide important information for land managers for post-fire runoff mitigation. This study concentrated on watersheds across the western US because this region includes a variety of forest types and watershed morphologies and is experiencing increased wildfire activity.

1.2 Objectives and Overview

The main objective of this study is to investigate wildfire effects on flood behavior in the 11 CONUS western states (Arizona, California, Colorado, Idaho, Montana, Nevada, New Mexico, Oregon, Utah, Washington, and Wyoming). This study investigated three aspects of post-fire flood behavior: normalized peak flows, the non-exceedance probability of peak flows, and runoff ratios for peak flow events. This study also focuses on testing a research hypothesis: For watersheds that experience wildfire, subsequent flood peaks within *X* years of that fire are statistically different from other flood samples. On the contrary, the null hypothesis is that flood peaks within *X* years after a wildfire event are simply random samples. To answer these research questions, the following subtasks were performed:

1) Acquire and pre-process the data, which include United States Geological Survey (USGS) annual peak flows, daily mean streamflows, North American Land Data Assimilation System version 2 (NLDAS-2) precipitation, NLDAS Variable Infiltration Capacity (NLDAS-VIC) simulated snowmelt, and Monitoring Trends in Burn Severity (MTBS) wildfire size and burn severity.
2) Analyze the unit peak flows (i.e., normalized by watershed sizes) for pre- and post-fire events and calculate their corresponding non-exceedance probability (NEP).
3) Calculate runoff ratios for historical peak flow events and compare results between pre- and post-fire events.
4) Derive the spatial distribution of changes in post-fire runoff ratios.

The results of this study are expected to serve as a guideline for the evaluation of wildfire effects on flood behavior and its persistence over the 11 CONUS western states. In addition, the regional wildfire impact information derived from this study can provide insights into post-fire floods at ungaged watersheds in different areas of the region. Future studies can incorporate this study into multivariate probability modeling (e.g., copula) and regional flood frequency analysis techniques to better understand the joint probability of extreme rainfall and post-fire flooding, as well as the impacts of these events on flood frequencies.

2. DATA

2.1 GAGES-II Watersheds and Their Annual Peak Flows

In this study, stream gages were identified using the Geospatial Attributes of Gages for Evaluating Streamflow version II (GAGES-II) dataset (Falcone 2011). The GAGES-II dataset provides a variety of features such as the geospatial boundary, elevation, geology, soils, and topography, anthropogenic influences for 9,322 stream gages within the CONUS. Of these stream gages, 3,089 are located within the 11 CONUS western states. A subset of 1,211 stream gages that conform to the following criteria were selected for this study:

1) Stream gages have at least 25 years of continuous annual peak flow data and at least 1 year of that period intersects the 1984-2020 period. This criterion can help maximize the number of watersheds where at least one wildfire event has occurred during the 1984-2020 period.
2) To exclude gages where streamflows are likely to be influenced by upstream reservoir operations, the upstream storage of the stream gages should not exceed 10,000 acre-feet (12.3 million m^3).
3) If multiple gages are located on the same stream, the drainage areas for the downstream gages must be at least twice that of the previous upstream gage.

For each watershed, the annual peak flow measurements (i.e., maximum instantaneous streamflow values for the entire water year from October 1st to September 30th) were collected from USGS stream gages using the "dataRetrieval" package in R computing language (Hirsch and De Cicco 2015).

2.2 Wildfire Data

To understand historical wildfire activities, satellite remote-sensing-based wildfire data were collected for the 1984-2020 period from the MTBS Project (Eidenshink et al. 2007). The MTBS dataset includes fire sizes (i.e., perimeters) larger than 1,000 acres in the western CONUS. Wildfire events were filtered out of the study dataset based on the following criteria: 1) not classified as either "wildfire" or "prescribed fire," and 2) not within the selected watersheds. This filtering resulted in a final dataset of 2,914 wildfire events over the western US during the 1984-2020 period.

2.3 Precipitation and Snowmelt Data

The event-scale runoff ratio was calculated using NLDAS-2 (Mitchell et al. 2004) observed precipitation and simulated snowmelt from the land surface model (NLDAS-VIC; Xia et al. 2012). Both the NLDAS-2 precipitation and NLDAS-VIC snowmelt datasets have hourly and 1/8° (roughly 12 km) spatial resolutions from 1979 to the present over the CONUS.

3. METHODS

3.1 Welch's *T*-test

Welch's *t*-test (i.e., the unequal variances *t*-test [Welch 1947]) is used to test the hypothesis that two populations have identical means. In this study, Welch's *t*-test was performed to compare the post-fire unit peak flows (i.e., peak flows divided by watershed size) with their pre-fire counterparts. The pre-fire peak flows are represented as all peak flows from 1 to 10 years before a wildfire, whereas the post-fire peak flows have five groups representing 1 to 5 years after a wildfire. For example, for all watersheds, the peak flows for the first year after a wildfire are defined as peak flows that occurred within 365 days after a wildfire. These values are compared against the corresponding watersheds' pre-fire peak flows that occurred 10 years before the wildfire at the earliest. Welch's *t*-tests were also performed for all watersheds in these groups with respect to different watershed burn area percentages (i.e., > 0 percent, > 25 percent, > 50 percent, and > 75 percent).

3.2 Non-exceedance Probabilities (NEPs) for Post-fire Peak Flows

It is widely accepted that the hydrologic impact of wildfire is relatively large within the initial years (e.g., one to five years) after a fire. Therefore, the NEPs of annual peak flows within five years of a wildfire are hypothesized to be larger than the corresponding values from a random sample. In this study, the probability of X randomly selected peak flows in which the NEPs are all larger than 0.5 was calculated using the following equation:

$$p(X) = \prod_{1}^{X} \frac{N}{2} * \frac{\frac{N}{2} - 1}{N - 1} \ldots * \frac{\frac{N}{2} - X + 1}{N - X + 1} \quad (1)$$

where X is the years after a wildfire and N is the total number of annual peak flows. For example, if a watershed has 50 years of continuous peak flow data, the probability of randomly selecting three samples (X=3) that are larger than the median value (i.e., rank 1 to 25) is:

$$p = \frac{25}{50} * \frac{24}{49} * \frac{23}{48} = 0.11735$$

This value is compared with the empirical probability that NEPs of peak flows within three years after a wildfire are > 0.5, which is defined as the ratio between the number of watersheds where peak flows within X year(s) after a wildfire are larger than the median value (i.e., NEP > 0.5) and the total number of watersheds that experienced wildfire.

3.3 Event-based Runoff Ratios

Because watershed sizes vary, the durations of peak flow events also vary. In this study, a single flood event is defined to be seven days, which includes the date of the annual peak flow occurrence as well as the three preceding and three subsequent days (Figure 1). The runoff ratio for flood peaks is therefore defined as:

$$r = \frac{Q_{total}}{P_{total}} \tag{2}$$

where Q_{total} is defined as the seven-day accumulated runoff depth and P_{total} is the accumulated precipitation and snowmelt total for the peak date and the three preceding days.

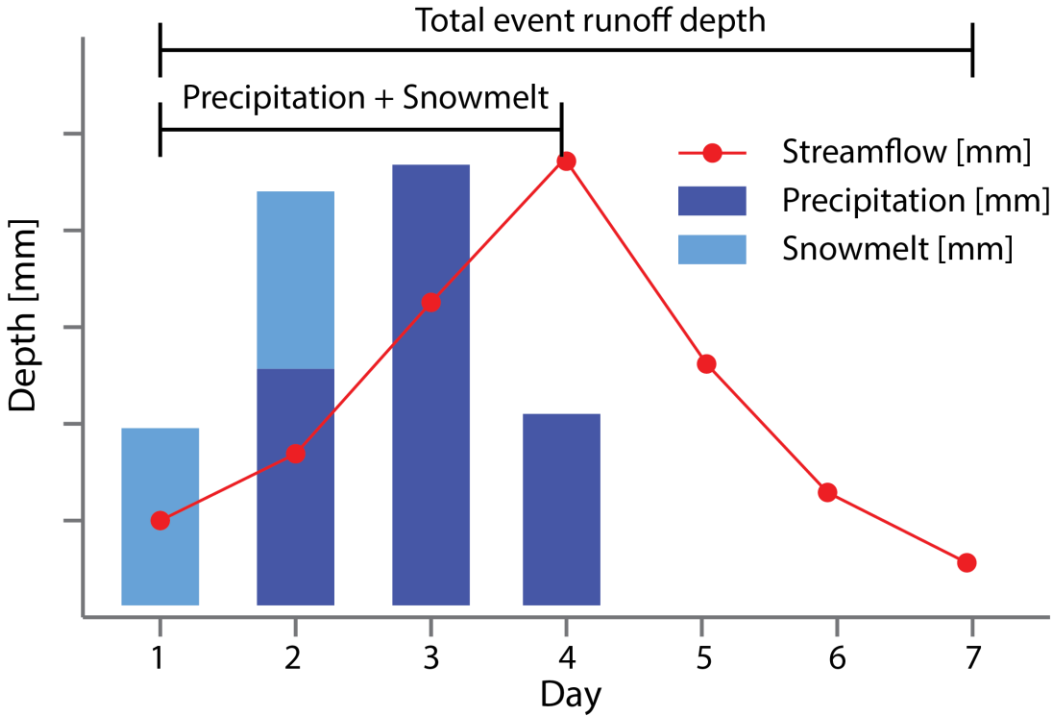

Figure 1. Schematic plot for calculation of runoff ratio.

4. RESULTS

4.1 Selected Watersheds and Their Historical Wildfires

In this study, 1,211 watersheds and 2,914 wildfire events over the western CONUS were selected based on the criteria in Section 2 (Figure 2a). These selected watersheds and wildfire events are spread across the 11 CONUS western states, which cover three main Köppen climate types: temperate, arid, and cold (Köppen 1884). All selected watersheds have more than 25 years of continuous annual peak flow records from the USGS gages and 50 percent have

annual peak flows of more than 50 continuous years (Figure 3a). Of the 1,211 watersheds, 497 (41 percent) have not experienced a wildfire event during the 1984-2020 period. These sites are predominantly located along the western front of the Cascade Range (i.e., western Washington and Oregon, Northern California, and central Colorado) where the long-term annual average precipitation is over 1,200 mm, which inhibits the occurrence of wildfire (Daly et al. 1997).

The remaining 714 watersheds (59 percent) have experienced at least one wildfire event during the period of concern, and most have experienced multiple wildfires (Figure 3b). For example, eight wildfire events have occurred in the Donner und Blitzen River watershed (518 km²) near Frenchglen, Oregon, from 1984 to 2020, with wildfire sizes ranging from 0.4 km² to 42 km² (Figure 2b). The burned area for the 714 watersheds with at least one wildfire ranges from 0.1 km² to over 4,000 km², with 90 percent between 1 km² and 1,000 km² (Figure 3c). The corresponding wildfire burned area (percent) with respect to watershed size is mostly less than 50 percent, with a few exceptions exceeding 75 percent of the watershed size (Figure 3d).

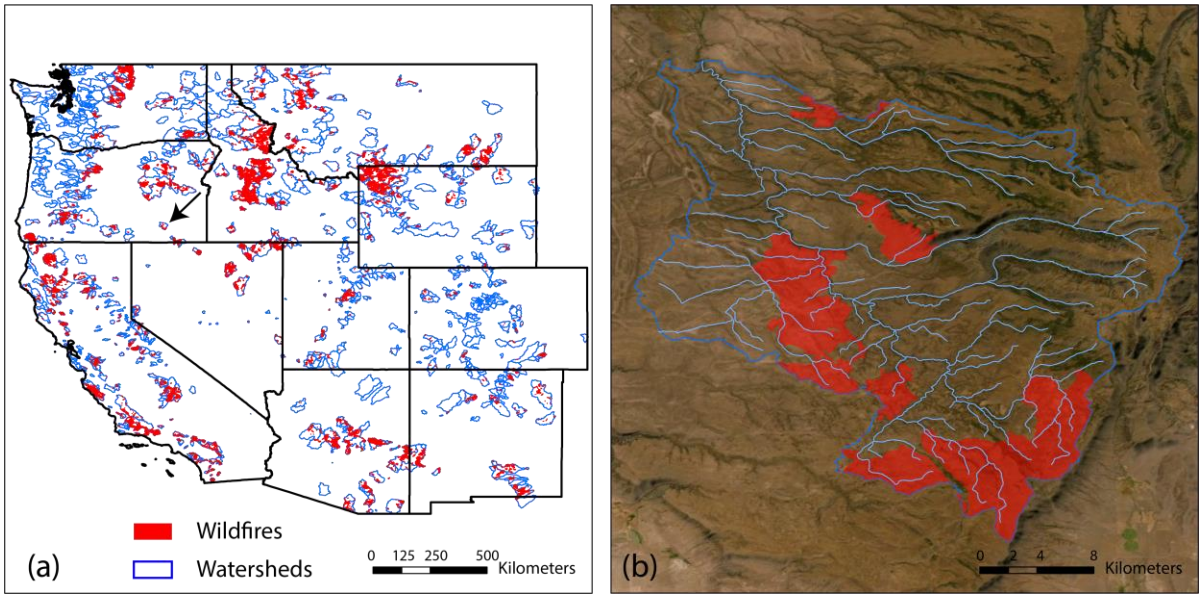

Figure 2. (a) The spatial distribution of the selected watersheds and the wildfires that occurred within these watersheds during the 1984-2020 period. The arrow in (a) points to the Donner und Blitzen River watershed near Frenchglen, Oregon, and (b) shows an example of the eight wildfires that occurred within that single watershed.

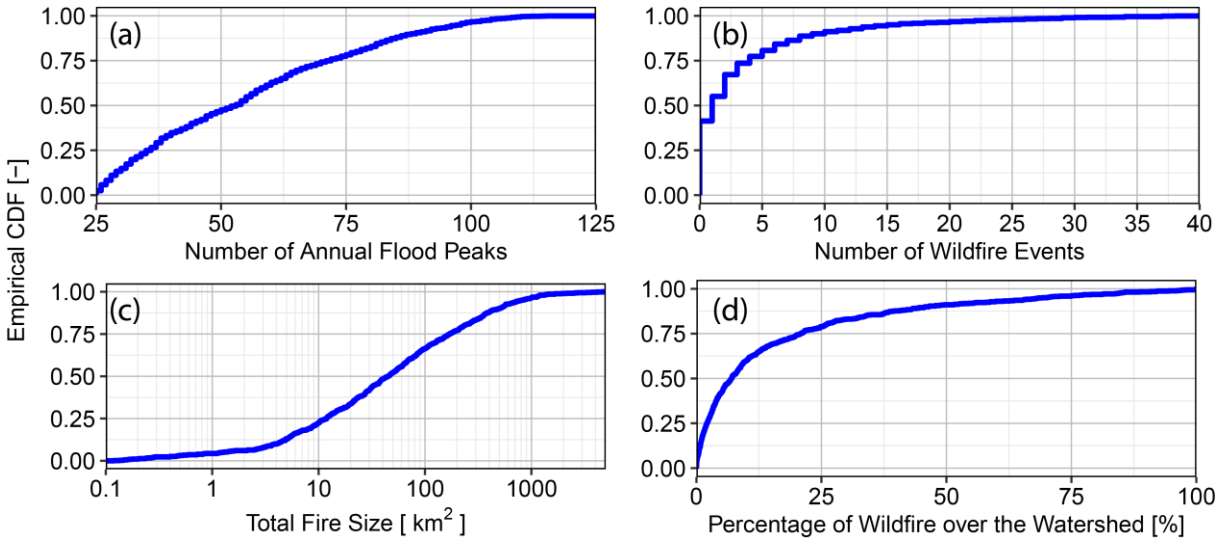

Figure 3. The empirical cumulative distribution functions (ECDFs) for (a) number of annual flood peaks, (b) number of wildfire events, (c) total wildfire size, and (d) the percentage of wildfire size over the watersheds for all watersheds across the western CONUS. If multiple wildfires have occurred in a watershed, the wildfire with the maximum size is used to calculate the percentage in (d).

Figure 4 provides similar information as Figure 3, but it reflects the spatial distributions of attributes in the selected watersheds and their corresponding wildfire events. In general, there is no systematic spatial bias present in the selected watersheds. For example, watersheds with either a large or small flood sample size are uniformly distributed over the western CONUS (Figure 4a). Similarly, watersheds with less than five wildfire events are also spread throughout the study region (Figure 4b). In addition, there is a strong correlation between wildfire size and percent burn area within the watersheds, with a Spearman's correlation coefficient equal to 0.9 (Figures 4c-d). Watersheds with a large wildfire size tend to cluster in three regions: the coast of California, southern Arizona, and the state of Idaho (Figures 4c-d).

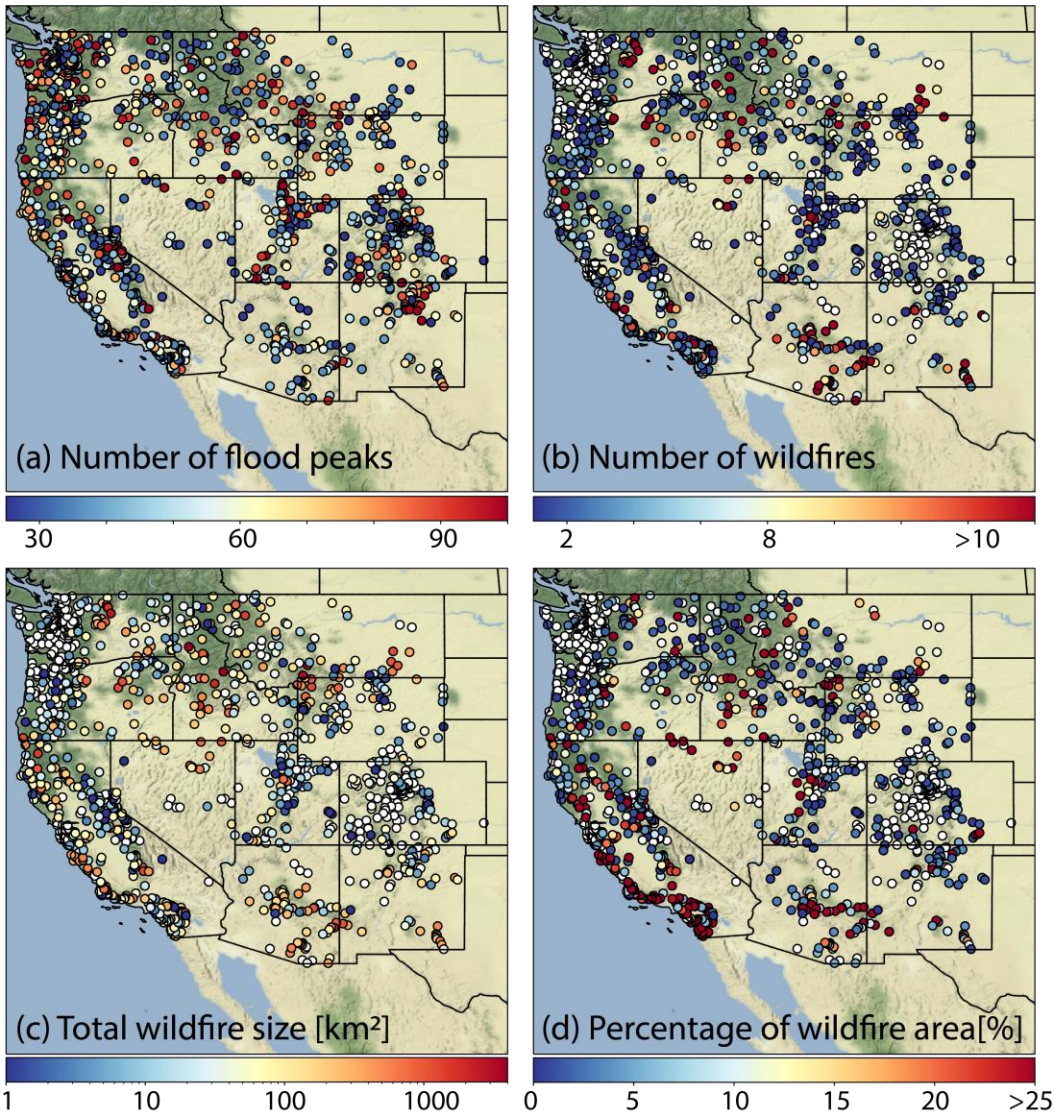

Figure 4. Spatial distribution of (a) flood samples and (b-d) wildfires. White dots in (b), (c), and
(d) denote the watersheds where wildfire did not occur within the period of concern.

4.2 The Seasonality of Wildfires and Floods

In general, both wildfire and flood events over the western CONUS reflect pronounced seasonality (Figure 5). Wildfire occurrence is predominantly between June and September with the peak season in early August, whereas floods have two distinct seasons: one between January and March and the other between May and July (Figures 5a-b). The wildfire season is uniformly distributed across the western CONUS because most wildfires occur during the summer (Figure 5a). In addition, wildfires in arid and semiarid regions—such as Arizona, Nevada, and New Mexico—typically occur approximately one to two months earlier than wildfire events in northern regions (Figure 5a).

Unlike the seasonality of wildfire, floods in the western CONUS have two dominant seasons associated with a marked spatial pattern. In general, floods occur in winter (e.g., January to

March) in the western coastal regions and in spring and summer in the interior regions (Figure 5b). This strong spatial pattern of flood seasonality in the western CONUS is attributable to the flood-generating mechanism. Floods in the western coastal regions are the result of winter stratiform precipitation, which is often associated with atmospheric rivers that transport moisture from the Pacific to this region (e.g., Ralph et al. 2006; Gershunov et al. 2017). Watersheds at high elevations (e.g., Rocky Mountains) and high latitudes (e.g., Montana) have a flood season in early summer due to snowmelt (Berghuijs et al. 2016). For the arid and semiarid southwestern CONUS, the North American Monsoon associated with local thunderstorms in late summer is the main flood driver (e.g., Higgins et al. 1997; Vivoni et al. 2006).

Because soil properties need time to recover after a wildfire event, the hydrologic impacts of wildfire on watersheds are typically greater in the period immediately following the wildfire and for a short period after. According to the difference in wildfire and flood seasonality, the interval between a wildfire and the first subsequent flood is extremely short for the Southwest (< 1 month), but it is approximately 5 and 10 months for the West Coast and high-latitude regions, respectively (Figure 5c). The short interval between a wildfire and the first subsequent flood for the Southwest can exacerbate the socioeconomic impact of post-fire floods and debris flows because of limited preparation time.

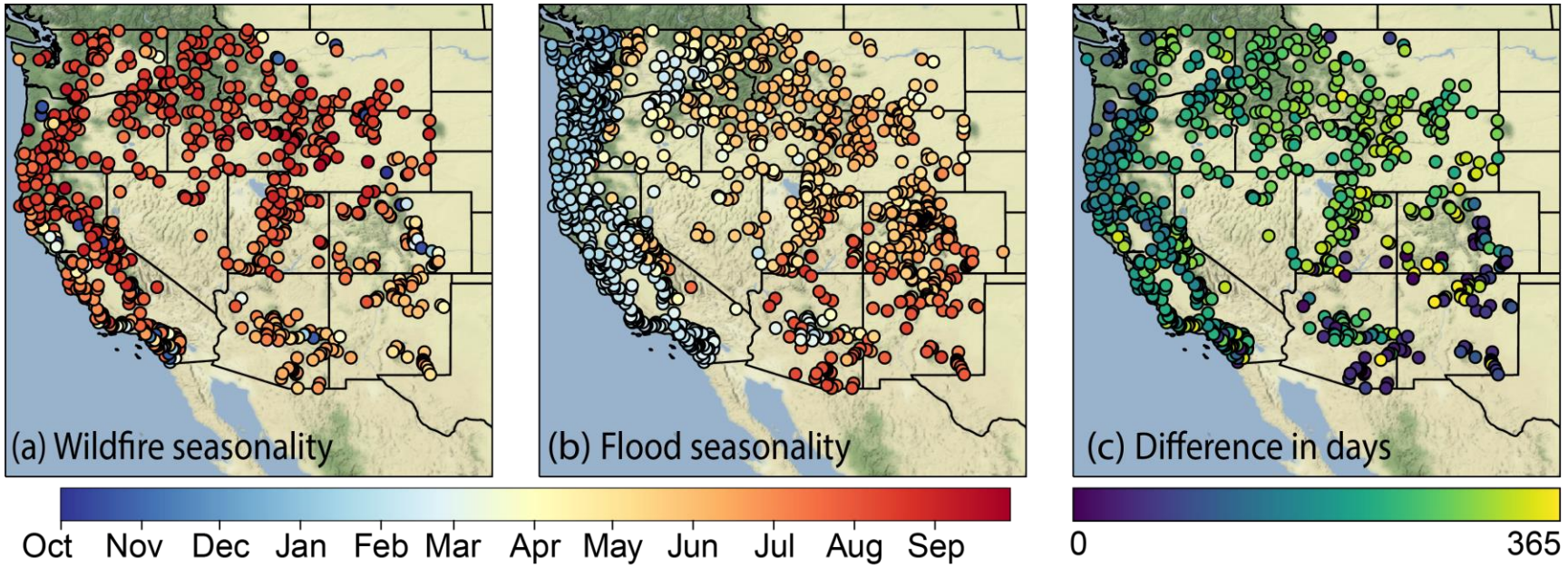

Figure 5. The seasonality of (a) wildfires and (b) annual peak flows, as well as (c) the difference between wildfire and flood seasonality.

4.3 Pre- and Post-fire Peak Flows and Their Non-exceedance Probabilities

Unit annual peak flows within both the 10 years before and after wildfires are defined as pre- and post-fire peak flows, respectively. Pre- and post-fire peak flows are grouped by the years before and after a wildfire and are analyzed with respect to different percent burn areas across watersheds (Figure 6 and Table 1). The wildfire impacts on peak flows become more pronounced with the increased percent burn area, although the sample size decreases (Figure 6). For watersheds that experienced at least a 25 percent burn area, their peak flows within the first year (< 365 days) of a wildfire are larger than the pre-fire peak flows (Figures 6b-d). The increases in post-fire peak flows are readily observable for the first three years after a wildfire and become less obvious five years after a wildfire (see the locally weighted scatterplot smoothing [LOWESS] regression in Figure 6). This pattern in post-fire peak flows is consistent with wildfire impacts on soil hydraulic properties that can last up to five years (Doerr et al. 2004, 2006; Malmon et al. 2007; Berg and Azuma 2010).

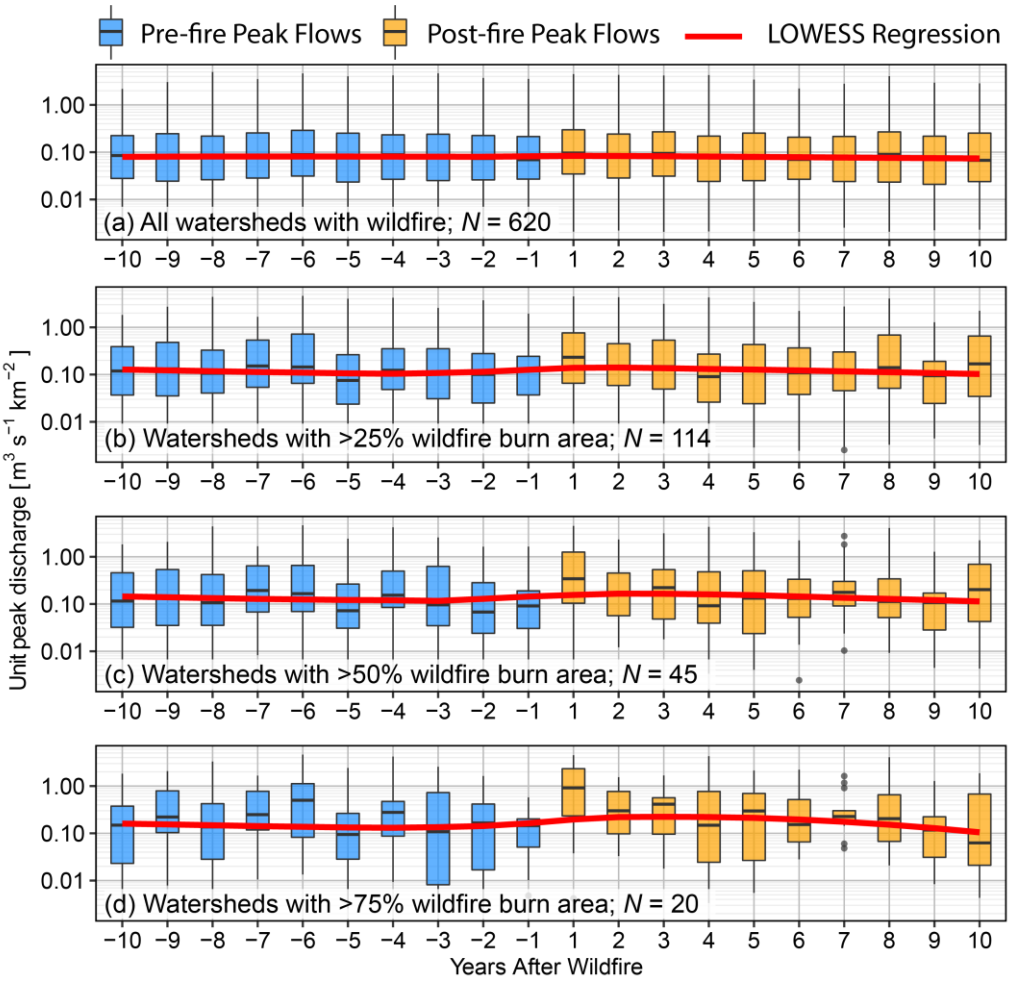

Figure 6. Pre- and post-fire unit peak flows (i.e., peak flows divided by watershed size) for watersheds with (a) > 0 percent, (b) > 25 percent, (c) > 50 percent, and (d) > 75 percent burn areas. Red lines denote the locally weighted scatterplot smoothing (LOWESS) regression fitted to unit peak flows, with smoothing parameter $\alpha = 1$. Sample sizes are given in each subplot.

Welch's *t*-test was also performed to compare the difference in mean pre- and post-fire peak flows with respect to different percent burn areas across the watersheds

(Table 1). The results show that irrespective of percent burn area, peak flows within the first year after a wildfire are significantly higher than pre-fire peak flows, with a *p*-value less than 0.05. In addition, the *p*-values of Welch's *t*-test generally increase with the years after a wildfire, indicating the failure to reject a null hypothesis of equal means in pre- and post-fire peak flows (Table 1).

For watersheds with > 0 percent burn area, there is more or less no change in the NEPs of post-fire peak flows. For watersheds with at least a 25 percent burn area, the changes in the NEPs of post-fire peak flows also show a similar pattern as in Figures 6b-d. The NEPs for peak flows within one year after a wildfire are generally greater than 0.5, meaning their magnitudes are larger than the median peak flows (Figure 7). The NEPs decrease in the second and third years after a wildfire, but the median values across the watersheds are still larger than 0.5. Irrespective of percent burn area, NEPs for the fourth year after a wildfire are less than 0.5, but then increase sharply above 0.5 in the fifth year. However, the physical cause for this change in peak flow NEP between the fourth and fifth year after a wildfire remains unknown.

Table 1. Welch's *t*-test for pre- and post-fire peak flows with respect to percent burn area. *T*-test value is shown for each group, with *p*-value shown in parentheses. Positive *t*-test values indicate that post-fire peak flows are larger than their pre-fire counterparts and vice versa for the negative *t*-test values. The pre-fire group is defined as all peak flows that occurred within 10 years before the wildfire.

Years After Wildfire	**Percentage Burn Area**			
	>0% (*N*=620)	**>25% (*N*=114)**	**>50% (*N*=45)**	**>75% (*N*=20)**
1	2.906 (0.004)*	3.065 (0.003)*	2.946 (0.005)*	2.973 (0.007)*
2	1.747 (0.081)	2.027 (0.045)*	1.215 (0.231)	1.302 (0.211)
3	0.442 (0.659)	0.243 (0.809)	-0.092 (0.927)	-0.826 (0.413)
4	-1.346 (0.179)	-0.366 (0.715)	0.270 (0.788)	0.4118 (0.685)
5	1.473 (0.141)	1.611 (0.111)	-0.149 (0.882)	-0.188 (0.852)

* Significant values (at five-percent level), indicating that there is a statistically significant difference in mean between two groups.

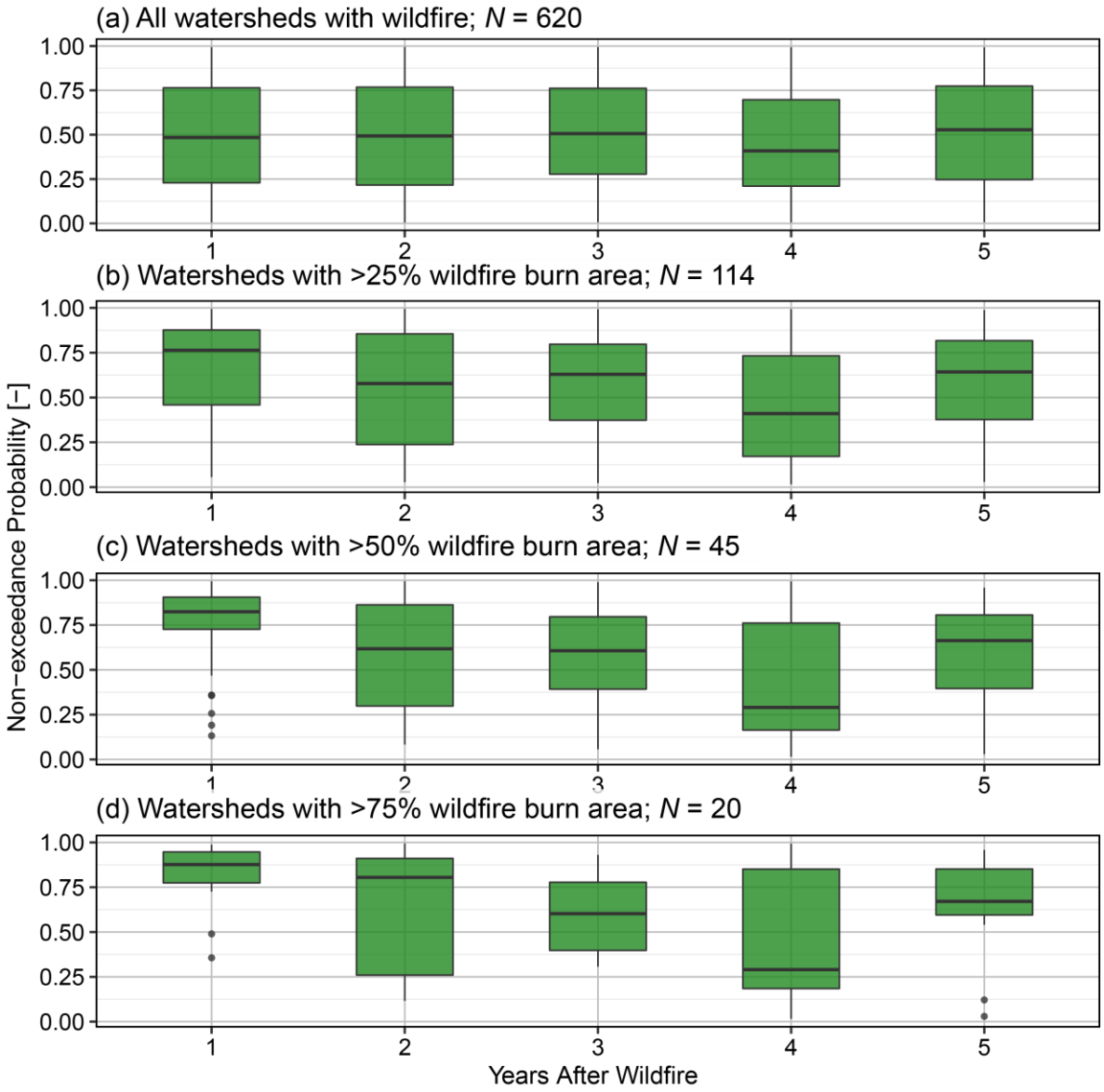

Figure 7. Non-exceedance probabilities for post-fire peak flows with respect to percent burn area. Percent burn areas and sample sizes are shown.

The probabilities of one to five consecutive annual peak flows after a wildfire that are both larger than their corresponding median peak flows (NEPs > 0.5) were calculated. These probabilities were compared with the probabilities of five randomly selected annual peak flows that are larger than the median values (Equation 1; Table 2). The results show that the probability of consecutive post-fire peak flows being larger than the median values (i.e., NEPs > 0.5) is slightly higher than the corresponding probability of random sampling.

Table 2. Comparison of the probability of X (i.e., 1-5) consecutive annual peak flows after a wildfire and randomly selected X annual peak flows that are all greater than their median values (i.e., NEPs > 0.5).

Years After Wildfire	Sample Size (i.e., number of watersheds)	NEPs of Flood Peaks > 0.5	
		Theoretical Value	Empirical Value
1	493	0.050	0.535
2	484	0.249	0.281
3	456	0.124	0.143
4	415	0.062	0.084
5	391	0.030	0.046

4.4 Post-fire Runoff Ratios

Runoff ratios for peak flows that occurred within one to five years after a wildfire (referred to as "post-fire runoff ratios" hereafter) were calculated for all available watersheds (Figures 8-12). Post-fire runoff ratios were compared to the watersheds' median runoff ratios. These comparisons were separated into four groups with respect to the watershed sizes: 1) watershed size < 162 km² (25th percentiles), 2) 162 km² ≤ watershed size < 405 km² (50th percentiles), 3) 405 km² ≤ watershed size < 983 km² (75th percentiles), and 4) watershed size > 983 km². In addition, the effects of the watersheds' mean annual precipitation (i.e., wetness) on such comparisons are accounted for.

In general, post-fire runoff ratios vary considerably with respect to watershed size. Small and medium watersheds (< 405 km²) experienced more marked hydrologic impacts of wildfires than large watersheds. For small watersheds, the post-fire runoff ratios, especially for the first three years after a wildfire, are typically higher than their median runoff ratios (Figures 8-10, panels a-b). However, relationships between the median and post-fire runoff ratios are more scattered for the large watersheds (Figures 8-10, panels c-d). This can be partly explained by the relative size differences between the watershed, wildfire burn, and storm cell. For small watersheds, there is a greater probability that the storms after a wildfire will overlap (i.e., hit) the same burn area, whereas this probability is low for large watersheds. For example, because the spatial scale of thunderstorms is approximately < 10 km², it is very likely such a storm may barely cover the burn area of a 1,000 km² watershed with a 10 percent burn area.

The hydrologic impacts of wildfires on peak flows are more pronounced for watersheds in dry climates (e.g., P_{annual} < 100 mm), especially during the first two years after a wildfire (Figures 8-9). Watersheds in arid and semiarid regions typically have low runoff ratios due to the dry initial soil moisture conditions, substantial channel transmission losses, and low hydrologic connectivity (McCuen 2002; Miller 2011; Smith et al. 2019). However, wildfires of a moderate to high burn severity can alter the soil structure and reduce hydraulic conductivity, leading to increased overland flow and higher flood peaks and volumes. In addition, severe thunderstorms are prevalent over arid and semiarid regions, especially

during the North American Monsoon (June 15th to the end of September). The interaction of these high-intensity thunderstorms with the low-infiltration-capacity soils caused by wildfire burns lead to runoff ratios which are higher than their median values.

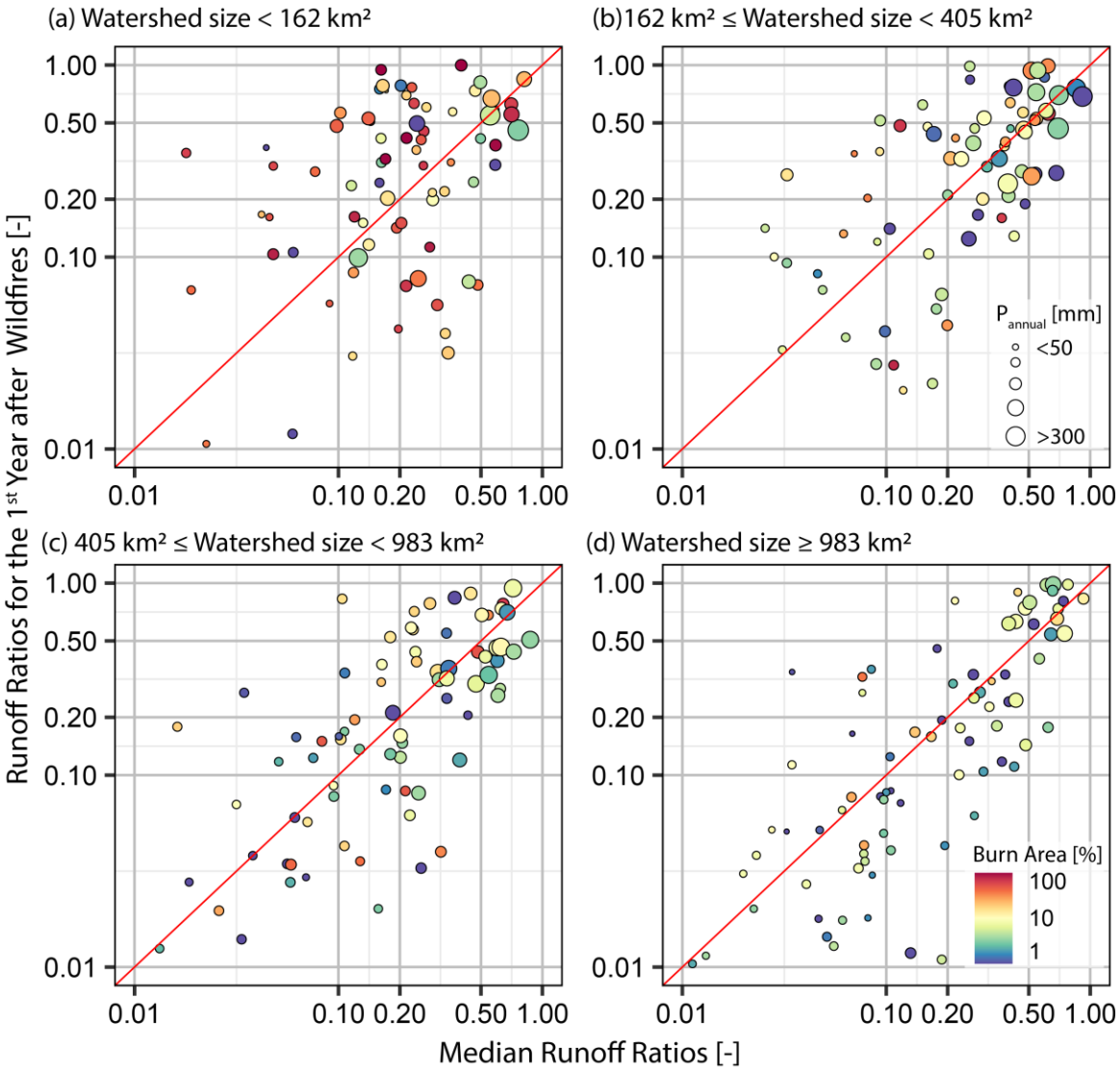

Figure 8. Relationships between watershed median runoff ratios and the corresponding values
for the first year after a wildfire. Scatter plots are grouped by the (a) 0-25th (162 km²),
(b) 25th-50th (405 km²), (c) 50th-75th (983 km²), and (d) 75th-100th percentiles of watershed size. Color and size of dots denote the percent burn area within watersheds and mean annual precipitation, respectively. Red lines denote a 1:1 relationship.

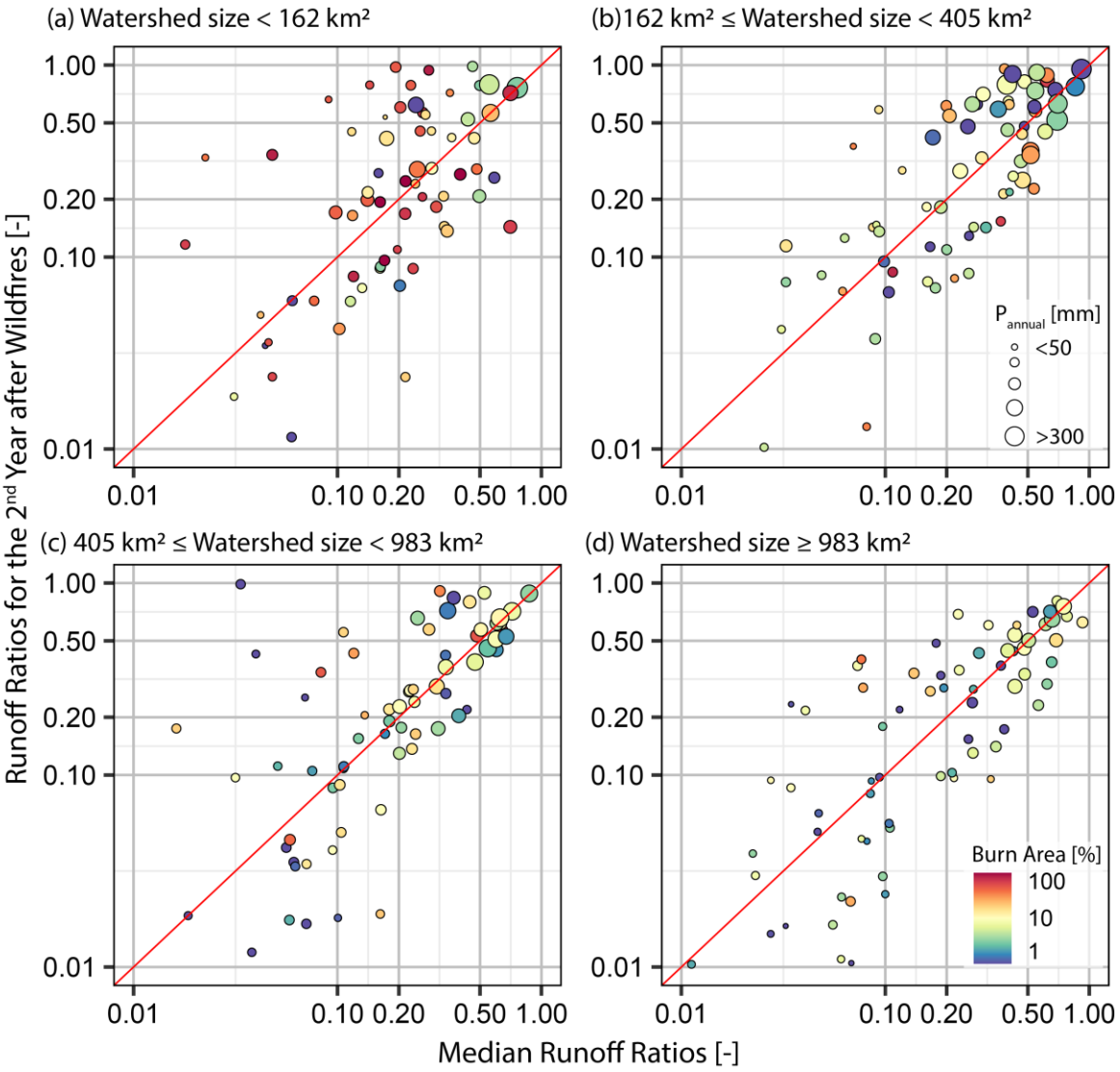

Figure 9. Relationships between watershed median runoff ratios and the corresponding values
for the second year after a wildfire. Scatter plots are grouped by the (a) 0-25th (162 km²), (b) 25th-50th (405 km²), (c) 50th-75th (983 km²), and (d) 75th-100th percentiles of watershed size. Color and size of dots denote the percent burn area within watersheds and mean annual precipitation, respectively. Red lines denote a 1:1 relationship.

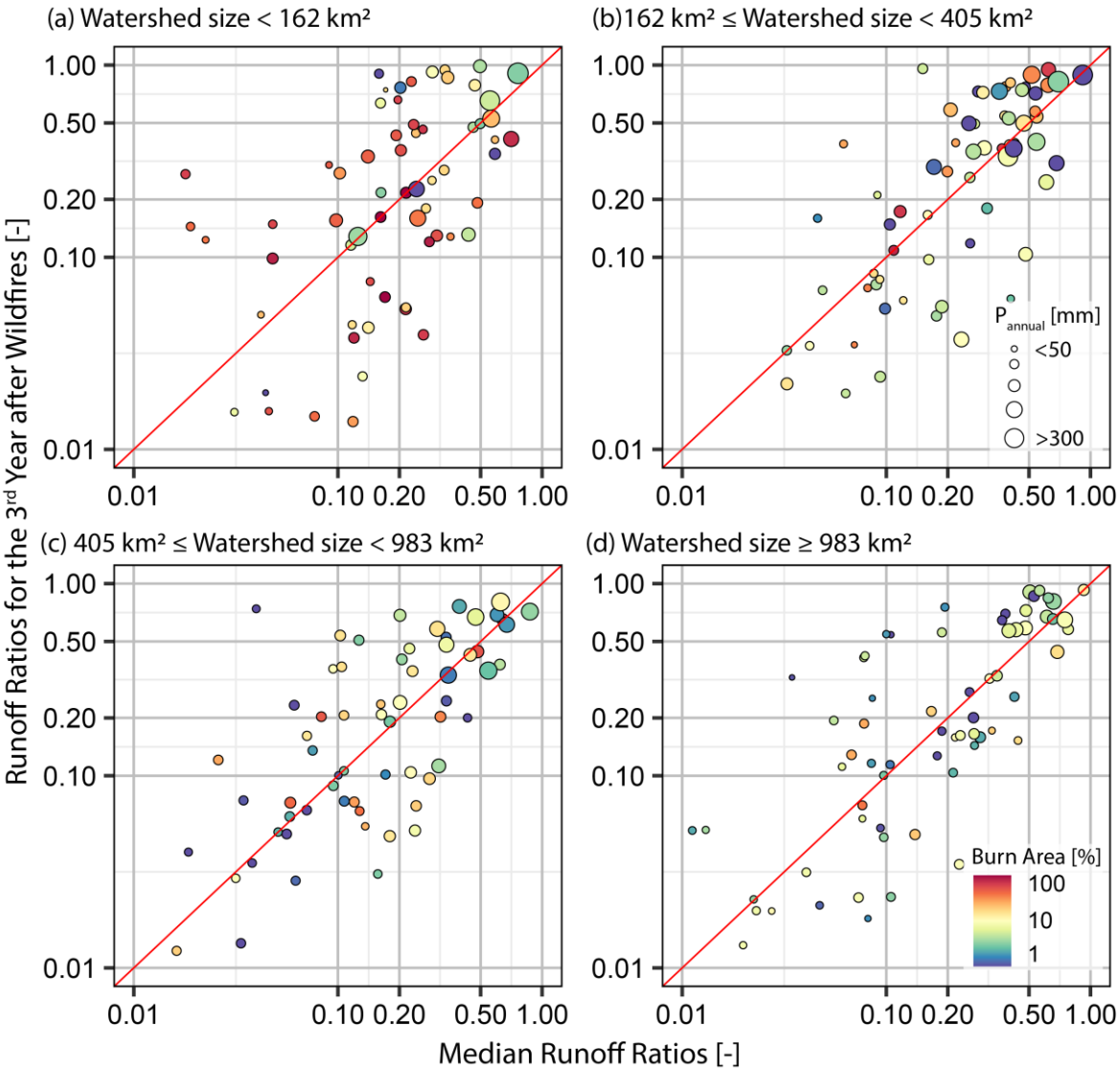

Figure 10. Relationships between watershed median runoff ratios and the corresponding values
for the third year after a wildfire. Scatter plots are grouped by the (a) 0-25th (162 km²), (b) 25th-50th (405 km²), (c) 50th-75th (983 km²), and (d) 75th-100th percentiles of watershed size. Color and size of dots denote the percent burn area within watersheds and mean annual precipitation, respectively. Red lines denote a 1:1 relationship.

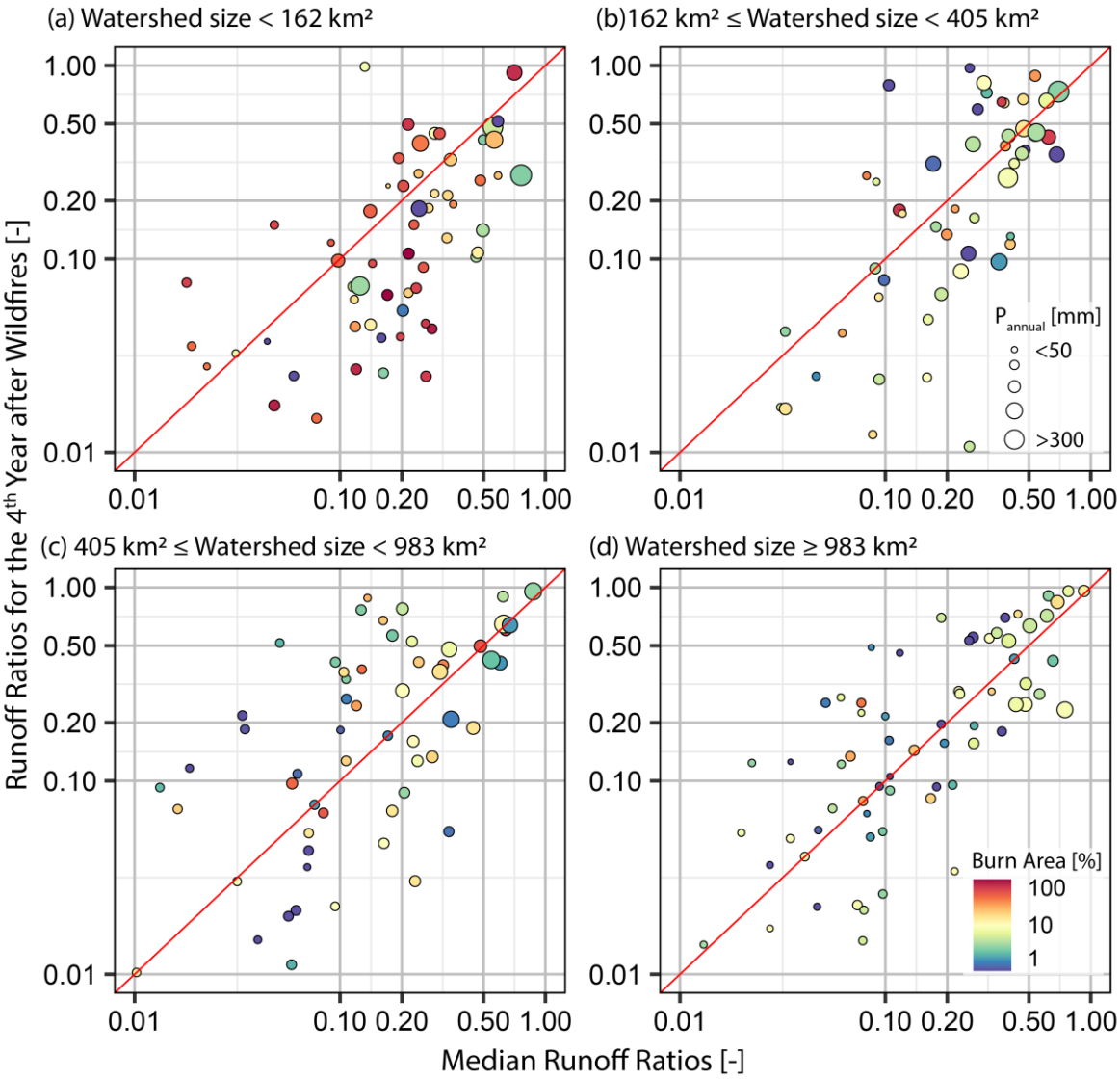

Figure 11. Relationships between watershed median runoff ratios and the corresponding values
for the fourth year after a wildfire. Scatter plots are grouped by the (a) 0-25th (162 km²), (b) 25th-50th (405 km²), (c) 50th-75th (983 km²), and (d) 75th-100th percentiles of watershed size. Color and size of dots denote the percent burn area within watersheds and mean annual precipitation, respectively. Red lines denote a 1:1 relationship.

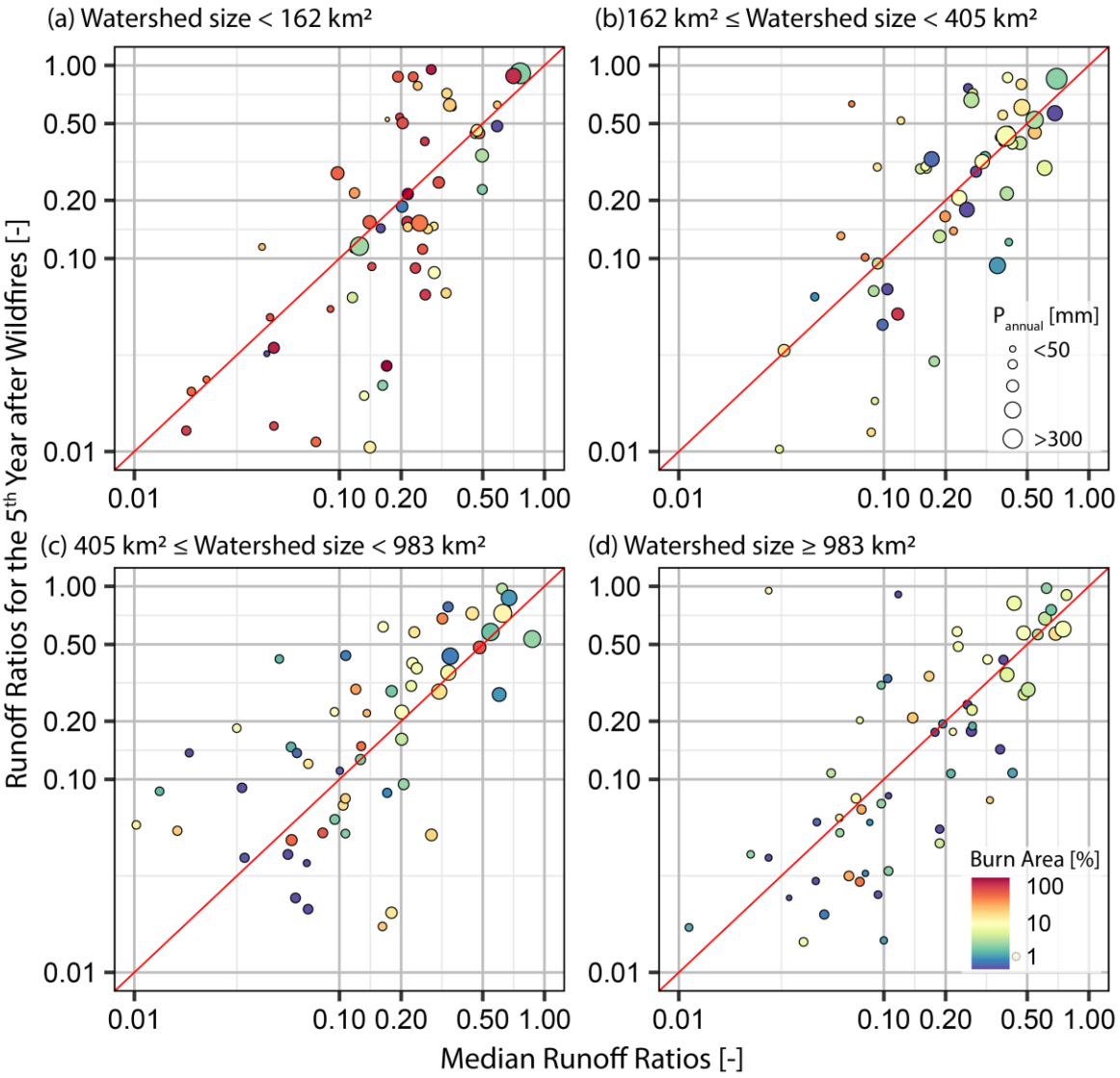

Figure 12. Relationships between watershed median runoff ratios and the corresponding values
for the fifth year after a wildfire. Scatter plots are grouped by the (a) 0-25th (162 km²), (b) 25th-50th (405 km²), (c) 50th-75th (983 km²), and (d) 75th-100th percentiles of watershed size. Color and size of dots denote the percent burn area within watersheds and mean annual precipitation, respectively. Red lines denote a 1:1 relationship.

The spatial distribution of post-fire runoff ratios is represented as the difference between runoff ratios for the first year after a wildfire and the corresponding median values (Figure 13). First, larger post-fire (i.e., within one year after a fire) runoff ratios are prevalent across the western US, especially for the Rocky Mountains and along the California coast. Second, the smaller the watershed size, the larger the post-fire runoff ratio. For most watersheds larger than 1,000 km², the post-fire runoff ratios are comparable to the median values.

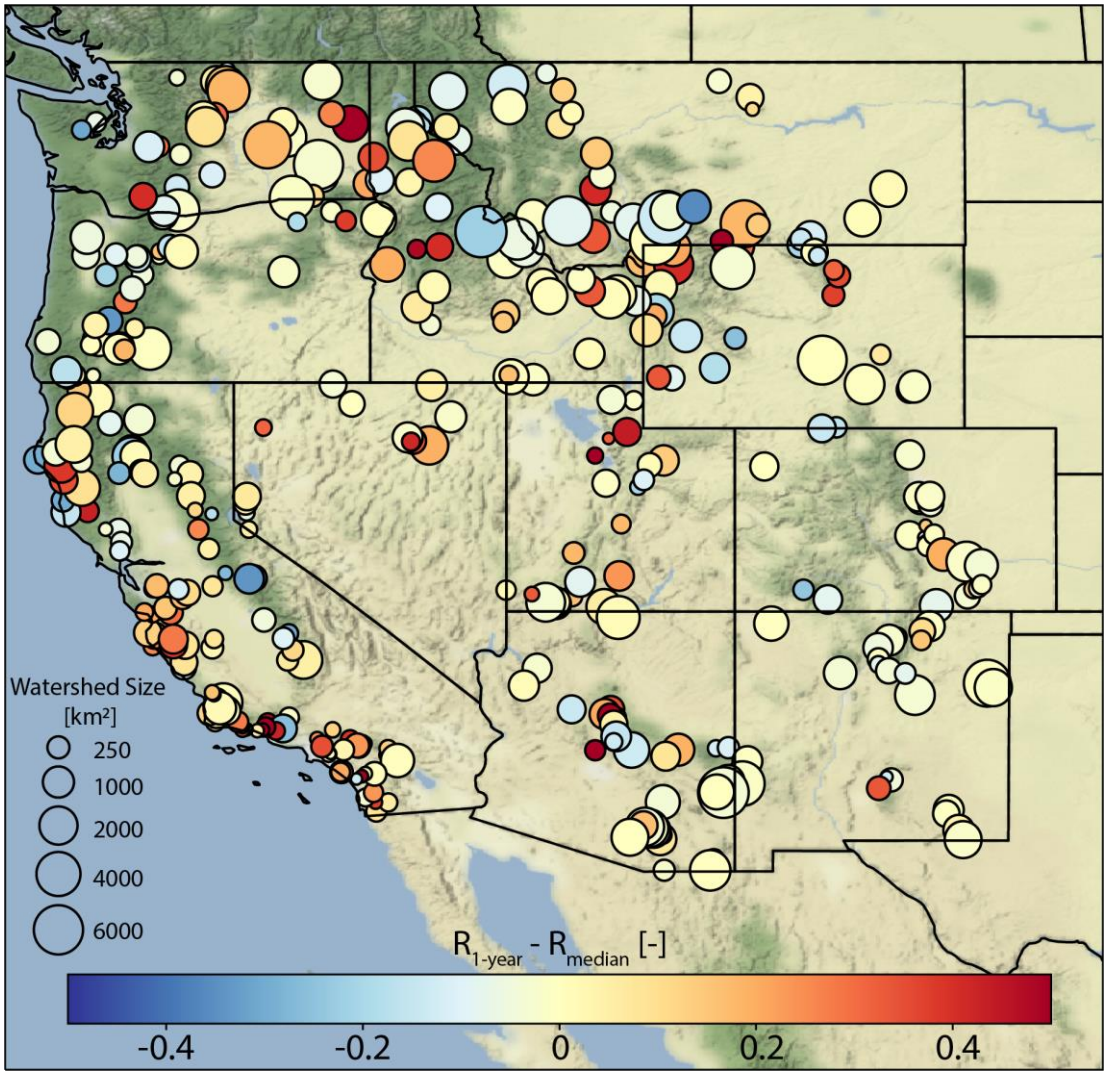

Figure 13. The difference in runoff ratios between the first year after a wildfire and the corresponding median values. Sizes of circles are proportional to the watershed sizes.

5. SUMMARY AND CONCLUSIONS

This study examined the impacts of wildfire on multiple aspects of flood behaviors for 714 watersheds across the western US. This study used a variety of observations and model simulations, including USGS annual peak flows, daily mean streamflows, NLDAS-2 precipitation, NLDAS-VIC simulated snowmelt, and MTBS wildfire size and burn severity. The combination of observations and simulations enables analyses of wildfire seasonality, changes in post-fire peak flows and their NEPs, and the comparison of pre- and post-fire runoff ratios for flood events. The major findings are as follows:

1) For 1,211 selected watersheds that have relatively minimal anthropogenic impacts, 714 watersheds (59 percent) have experienced at least one wildfire event during the 1984-2020 period, with sizes ranging from less than 1 km² to over 1,000 km². These 714 watersheds show disparate seasonalities between

wildfire and floods associated with their geographical locations. The interval between a wildfire and the first subsequent flood is longest (~ 10 months) for high-latitude states, relatively short (~ 5 months) for the West Coast, and shortest (< 1 month) for the arid Southwest.

2) For all watersheds that experienced wildfires during the 1984-2020 period, the unit annual peak flows (i.e., peak flows divided by watershed sizes) within both 10 years before and after wildfires were analyzed. Peak flows for the first year after a wildfire are statistically significantly larger than the pre-fire peak flows. This pattern is more pronounced for watersheds with larger percent burn areas and continues for the first three years after a wildfire. This result implies that wildfire impacts on peak flows are dynamic processes related to the soil and vegetation recovery pattern.

3) The NEPs for post-fire peak flows are generally greater than 0.5 for the first three years after a wildfire, especially for the watersheds with > 25 percent burn area. This indicates post-fire peak flows within three years are larger than their median flood peaks irrespective of other flood drivers, such as rainfall and initial soil moisture (Figure 7). For the watersheds showing post-fire increases in NEPs, the hypothesis that post-fire floods have the same mean value as pre-fire NEP's can be rejected.

4) Runoff ratios for floods within one to five years after a wildfire were compared with their median peak flow runoff ratios. For small and medium watersheds (< 405 km^2), post-fire runoff ratios are higher than their median values, especially for the first year after a wildfire. This phenomenon is more prevalent among watersheds in arid regions with annual precipitation less than 100 mm. For large watersheds (> 405 km^2), the relationship between post-fire and median runoff ratios is more scattered.

It has been acknowledged that wildfire processes affect peak runoff in the post-fire period, but results to date have been focused on individual events in individual basins. There is large uncertainty in the factors that have the greatest influence on increased peak flows and the time it takes for the basin to revert to peak flows of the same magnitude as pre-fire conditions. This study further demonstrates the complexity of changes in post-fire peak flows with respect to time, different watershed sizes, and the percent burn area. It also shows that the impacts of wildfire on peak flows are the strongest within the first one to three years after a fire, and then lessen after four to five years. The empirical analyses performed in this study have wide-ranging implications for better understanding post-fire flood risk. For example, post-fire flood frequency analysis should account for impacts across the fire continuum rather than just a single wildfire event.

REFERENCES

Abatzoglou, J. T., and A. P. Williams, 2016: Impact of anthropogenic climate change on wildfire across western US forests. *Proc Natl Acad Sci USA*, **113**, 11770–11775, https://doi.org/10.1073/pnas.1607171113.

Aronica, G., A. Candela, and M. Santoro, 2002: Changes in the hydrological response of two Sicilian basins affected by fire. *FRIEND 2002 - regional hydrology: bridging the gap between research and practice. Fourth International Conference on FRIEND (Flow Regimes from International Network Data), Cape Town, South Africa, 18-22 March 2002*, 163–169.

Bart, R., and A. Hope, 2010: Streamflow response to fire in large catchments of a Mediterranean-climate region using paired-catchment experiments. *Journal of Hydrology*, **388**, 370–378, https://doi.org/10.1016/j.jhydrol.2010.05.016.

Benavides-Solorio, J., and L. H. MacDonald, 2001: Post-fire runoff and erosion from simulated rainfall on small plots, Colorado Front Range. *Hydrological Processes*, **15**, 2931–2952, https://doi.org/10.1002/hyp.383.

Berg, N. H., and D. L. Azuma, 2010: Bare soil and rill formation following wildfires, fuel reduction treatments, and pine plantations in the southern Sierra Nevada, California, USA. *International Journal of Wildland Fire. 19(4): 478-489*, **19**, 478–489.

Berghuijs, W. R., R. A. Woods, C. J. Hutton, and M. Sivapalan, 2016: Dominant flood generating mechanisms across the United States. *Geophysical Research Letters*, **43**, 4382–4390, https://doi.org/10.1002/2016GL068070.

Cannon, S. H., R. M. Kirkham, and M. Parise, 2001: Wildfire-related debris-flow initiation processes, Storm King Mountain, Colorado. *Geomorphology*, **39**, 171–188, https://doi.org/10.1016/S0169-555X(00)00108-2.

Coombs, J. S., and J. M. Melack, 2013: Initial impacts of a wildfire on hydrology and suspended sediment and nutrient export in California chaparral watersheds: WILDFIRE IMPACTS ON HYDROLOGY AND EXPORT. *Hydrol. Process.*, **27**, 3842–3851, https://doi.org/10.1002/hyp.9508.

Daly, C., G. H. Taylor, and W. P. Gibson, 1997: The PRISM approach to mapping precipitation and temperature. *Proc., 10th AMS Conf. on Applied Climatology*, Citeseer, 20–23.

DeBano, L. F., L. D. Mann, and D. A. Hamilton, 1970: Translocation of Hydrophobic Substances into Soil by Burning Organic Litter. *Soil Science Society of America Journal*, **34**, 130–133, https://doi.org/10.2136/sssaj1970.03615995003400010035x.

DeBano, L. F., R. M. Rice, and C. C. Eugene, 1979: Soil heating in chaparral fires: effects on soil properties, plant nutrients, erosion, and runoff. *Res. Paper PSW-RP-145. Berkeley, CA: U.S. Department of Agriculture, Forest Service, Pacific Southwest Forest and Range Experiment Station. 21 p*, **145**.

Doerr, S. H., and Coauthors, 2004: Heating effects on water repellency in Australian eucalypt forest soils and their value in estimating wildfire soil temperatures. *Int. J. Wildland Fire*, **13**, 157–163, https://doi.org/10.1071/WF03051.

Doerr, S. H., R. A. Shakesby, W. H. Blake, C. J. Chafer, G. S. Humphreys, and P. J. Wallbrink, 2006: Effects of differing wildfire severities on soil wettability and implications for hydrological response. *Journal of Hydrology*, **319**, 295–311, https://doi.org/10.1016/j.jhydrol.2005.06.038.

Ebel, B. A., and J. A. Moody, 2013: Rethinking infiltration in wildfire-affected soils. *Hydrological Processes*, **27**, 1510–1514, https://doi.org/10.1002/hyp.9696.

Eidenshink, J., B. Schwind, K. Brewer, Z.-L. Zhu, B. Quayle, and S. Howard, 2007: A Project for Monitoring Trends in Burn Severity. *fire ecol*, **3**, 3–21, https://doi.org/10.4996/fireecology.0301003.

Falcone, J. A., 2011: *GAGES-II: Geospatial attributes of gages for evaluating streamflow*. US Geological Survey.

Gershunov, A., T. Shulgina, F. M. Ralph, D. A. Lavers, and J. J. Rutz, 2017: Assessing the climate-scale variability of atmospheric rivers affecting western North America. *Geophysical Research Letters*, **44**, 7900–7908, https://doi.org/10.1002/2017GL074175.

Higgins, R. W., Y. Yao, and X. L. Wang, 1997: Influence of the North American Monsoon System on the U.S. Summer Precipitation Regime. *Journal of Climate*, **10**, 2600–2622, https://doi.org/10.1175/1520-0442(1997)010<2600:IOTNAM>2.0.CO;2.

Hirsch, R. M., and L. A. De Cicco, 2015: *User guide to Exploration and Graphics for RivEr Trends (EGRET) and dataRetrieval: R packages for hydrologic data*. Version 1.0: Originally posted October 8, 2014; Version 2.0: February 5, 2015.

Imeson, A. C., J. M. Verstraten, E. J. van Mulligen, and J. Sevink, 1992: The effects of fire and water repellency on infiltration and runoff under Mediterranean type forest. *CATENA*, **19**, 345–361, https://doi.org/10.1016/0341-8162(92)90008-Y.

Jay, A., and Coauthors, 2018: *Chapter 1 : Overview. Impacts, Risks, and Adaptation in the United States: The Fourth National Climate Assessment, Volume II*. U.S. Global Change Research Program.

Kinoshita, A. M., and T. S. Hogue, 2015: Increased dry season water yield in burned watersheds in Southern California. *Environ. Res. Lett.*, **10**, 014003, https://doi.org/10.1088/1748-9326/10/1/014003.

Köppen, W., 1884: Die Wärmezonen der Erde, nach der Dauer der heissen, gemässigten und kalten Zeit und nach der Wirkung der Wärme auf die organische Welt betrachtet. *Meteorologische Zeitschrift*, 215–226.

Loáiciga, H. A., D. Pedreros, and D. Roberts, 2001: Wildfire-streamflow interactions in a chaparral watershed. *Advances in Environmental Research*, **5**, 295–305, https://doi.org/10.1016/S1093-0191(00)00064-2.

Malmon, D. V., S. L. Reneau, D. Katzman, A. Lavine, and J. Lyman, 2007: Suspended sediment transport in an ephemeral stream following wildfire. *Journal of Geophysical Research: Earth Surface*, **112**, https://doi.org/10.1029/2005JF000459.

McCuen, R. H., 2002: *Modeling Hydrologic Change: Statistical Methods*. CRC Press, 448 pp.

Meyer, G. A., J. L. Pierce, S. H. Wood, and A. J. T. Jull, 2001: Fire, storms, and erosional events in the Idaho batholith. *Hydrological Processes*, **15**, 3025–3038, https://doi.org/10.1002/hyp.389.

Miller, J. J., 2011: Geologic and Hydraulic Concepts of Arid Environments. *Flood Hazard Identification and Mitigation in Semi- and Arid Environments*, WORLD SCIENTIFIC, 19–35.

Mitchell, K. E., and Coauthors, 2004: The multi-institution North American Land Data Assimilation System (NLDAS): Utilizing multiple GCIP products and partners in a continental distributed hydrological modeling system. *Journal of Geophysical Research: Atmospheres*, **109**.

Moody, J. A., and B. A. Ebel, 2012: Hyper-dry conditions provide new insights into the cause of extreme floods after wildfire. *CATENA*, **93**, 58–63, https://doi.org/10.1016/j.catena.2012.01.006.

——, R. A. Shakesby, P. R. Robichaud, S. H. Cannon, and D. A. Martin, 2013: Current research issues related to post-wildfire runoff and erosion processes. *Earth-Science Reviews*, **122**, 10–37, https://doi.org/10.1016/j.earscirev.2013.03.004.

Neary, D. G., K. C. Ryan, and L. F. DeBano, 2005: Wildland fire in ecosystems: effects of fire on soils and water. *Gen. Tech. Rep. RMRS-GTR-42-vol.4. Ogden, UT: U.S. Department of Agriculture, Forest Service, Rocky Mountain Research Station. 250 p.*, **042**, https://doi.org/10.2737/RMRS-GTR-42-V4.

NIFC, 2020: *Historical Wildland Fire Information and Federal Firefighting Costs*. National Interagency Fire Center, https://www.nifc.gov/fireInfo/fireInfo_documents/SuppCosts.pdf.

Onda, Y., W. E. Dietrich, and F. Booker, 2008: Evolution of overland flow after a severe forest fire, Point Reyes, California. *CATENA*, **72**, 13–20, https://doi.org/10.1016/j.catena.2007.02.003.

Ralph, F. M., P. J. Neiman, G. A. Wick, S. I. Gutman, M. D. Dettinger, D. R. Cayan, and A. B. White, 2006: Flooding on California's Russian River: Role of atmospheric rivers. *Geophysical Research Letters*, **33**, https://doi.org/10.1029/2006GL026689.

Scott, D. F., and D. B. Van Wyk, 1990: The effects of wildfire on soil wettability and hydrological behaviour of an afforested catchment. *Journal of Hydrology*, **121**, 239–256, https://doi.org/10.1016/0022-1694(90)90234-O.

Smith, J. A., M. L. Baeck, L. Yang, J. Signell, E. Morin, and D. C. Goodrich, 2019: The Paroxysmal Precipitation of the Desert: Flash Floods in the Southwestern United States. *Water Resources Research*, **55**, 10218–10247, https://doi.org/10.1029/2019WR025480.

Townsend, S. A., and M. M. Douglas, 2000: The effect of three fire regimes on stream water quality, water yield and export coefficients in a tropical savanna (northern Australia). *Journal of Hydrology*, **229**, 118–137, https://doi.org/10.1016/S0022-1694(00)00165-7.

Vivoni, E. R., R. S. Bowman, R. L. Wyckoff, R. T. Jakubowski, and K. E. Richards, 2006: Analysis of a monsoon flood event in an ephemeral tributary and its downstream hydrologic effects. *Water Resources Research*, **42**, https://doi.org/10.1029/2005WR004036.

Welch, B. L., 1947: THE GENERALIZATION OF 'STUDENT'S' PROBLEM WHEN SEVERAL DIFFERENT POPULATION VARLANCES ARE INVOLVED. *Biometrika*, **34**, 28–35, https://doi.org/10.1093/biomet/34.1-2.28.

Westerling, A. L., H. G. Hidalgo, D. R. Cayan, and T. W. Swetnam, 2006: Warming and Earlier Spring Increase Western U.S. Forest Wildfire Activity. *Science*, **313**, 940–943, https://doi.org/10.1126/science.1128834.

Xia, Y., and Coauthors, 2012: Continental-scale water and energy flux analysis and validation for the North American Land Data Assimilation System project phase 2 (NLDAS-2): 1. Intercomparison and application of model products. *Journal of Geophysical Research: Atmospheres*, **117**, https://doi.org/10.1029/2011JD016048.